RESEARCH ARTICLE

Antibacterial Potential of Nanogels Containing Bergamot, Pine, and Mixed Essential Oils

Farzane Dianat[1,2], Erfan Azadifar[3], Roghayeh Heiran[4], Elham Rostami[3], Zahra Montaseri[5*], Mahmoud Osanloo[6*]

[1] Student Research Committee, Fasa University of Medical Sciences, Fasa, Iran

[2] Department of Medicine, School of Medicine, Fasa University of Medical Sciences, Fasa, Iran

[3] Department of Medical Biotechnology, School of Advanced Technologies in Medicine, Fasa University of Medical Sciences, Fasa, Iran

[4] Estahban Higher Education Center- Shiraz University, Estahban, Iran

[5] Department of Infectious Diseases, School of Medicine, Fasa University of Medical Sciences, Fasa, Iran

[6] Department of Medical Nanotechnology, School of Advanced Technologies in Medicine, Fasa University of Medical Sciences, Fasa, Iran

ARTICLE INFO

Article History:
Received 12 Oct 2024
Accepted 25 Jan 2025
Published 01 Mar 2025

Keywords:
Citrus bergamia
Pinus sylvestris
Herbal Medicine
Antibacterial activity

ABSTRACT

Bacterial skin infection is a common clinical condition that impacts different organs. The emergence of antibiotic resistance is due to the overuse of antibiotics, which is rapidly increasing in developing countries. Due to the antibacterial properties of medical plants, they could be used as a treatment against various diseases like infectious diseases. The chemical composition of bergamot and pine essential oil (EO) was first investigated using GC-MS analysis. Nanoemulsion-based gels containing bergamot, pine, and a mixture of these EOs were then prepared. The viscosity of the nanogels was measured by viscometry. Attenuated total reflectance Fourier-transform infrared (ATR-FTIR) spectroscopy was employed to confirm the successful encapsulation of EOs within the nanogel matrix. Furthermore, the antibacterial effects of nanogels were investigated against *Escherichia coli* (Gram-negative) and *Staphylococcus aureus* (Gram-positive) using the AATCC100 method. Linalool (48.50%), limonene (21.24%), linalool acetate (17.37%), α-terpineol (5.70%), and geranyl acetate (1.74%) were identified as significant bergamot compounds EO. The major constituents of pine EO were α-terpineol (66.69%), γ-terpineol (13.10%), terpinen-1-ol (11.15%), cis-β-terpineol (3.00%), and terpinen-4-ol (2.09%). The particle size of nanoemulsion containing bergamot EO, pine EO, and their mixture was measured as 34 ± 4 nm, 10 ± 2 nm, and 42 ± 6 nm, respectively. The viscosity of nanogels was fully fitted to the Carreau-Yasuda model. Interestingly, pine nanogel at 2000 µg/mL exhibited 95% growth inhibition against E. coli and S. aureus. Pine nanogel exhibited a favorable antibacterial effect against E. coli and S. aureus, so that it could be considered for further antibacterial investigation.

How to cite this article
Dianat F., Azadifar E., Heiran R., Rostami E., Montaseri Z., Osanloo M. Antibacterial Potential of Nanogels Containing Bergamot, Pine, and Mixed Essential Oils. Nanomed Res J, 2024; 10(1): 70-80. DOI: 10.22034/nmrj.2025.01.008

INTRODUCTION

The skin, the largest organ in the human body, is a crucial barrier in the immune system, preventing pathogenic microorganisms from invading underlying tissues [1, 2]. However, skin injuries or immune dysfunction can facilitate microbial invasion, leading to infections such as impetigo, cellulitis, and folliculitis, which are particularly common among hospitalized patients [3, 4]. Among bacterial pathogens, *Staphylococcus aureus*, a gram-positive bacterium, readily colonizes keratinocytes and causes various cutaneous infections, including abscesses, cellulitis, and impetigo [5, 6]. Similarly, *Escherichia coli*, a gram-negative bacterium, can also contribute to skin and soft tissue infections [7, 8].

* Corresponding Author Email: *osanloo_mahmood@yahoo.com*
montaserizahra90@gmail.com

Despite the effectiveness of antibiotics in treating bacterial infections, their administration can lead to severe side effects, such as leukopenia, thrombocytopenia, anemia, drug fever, and encephalopathy [9, 10]. Furthermore, the rising incidence of antibiotic resistance, particularly in *S. aureus* and *E. coli*, poses a significant global health challenge, with developing countries bearing a disproportionate burden [11, 12]. These limitations have intensified the search for alternative antimicrobial therapies.

Medicinal plants have long been utilized for their therapeutic properties, offering a sustainable source of bioactive compounds with antimicrobial activity [13, 14]. Their affordability, accessibility, and safety make them promising candidates for the treatment of infections. *Citrus bergamia* (bergamot), a member of the *Rutaceae* family native to southern Italy, exhibits antimicrobial properties, particularly against gram-negative bacteria [15, 16]. Similarly, *Pinus sylvestris* (Scots pine), a widely distributed species in Eurasia, demonstrates antibacterial, antiviral, and antifungal effects [17, 18].

Despite their promising antimicrobial properties, essential oils (EOs) face challenges in therapeutic applications due to their volatility and susceptibility to degradation [19]. Incorporating EOs into hydrogel matrices is an effective strategy to modulate their hydrophobicity and enhance stability. Hydrogels are polymeric networks that can disperse drugs within their matrix. Recently, a novel type of hydrogel—nanostructured hydrogels based on nanoemulsions, sometimes called emulgels—has been developed [20, 21]. Nanoemulsions are thermodynamically stable colloidal systems with droplet sizes typically below 200 nm. They offer several advantages in drug delivery, including enhanced solubility of hydrophobic compounds, improved bioavailability, and controlled release properties. Moreover, nanoemulsions enhance the penetration of active ingredients through biological barriers, making them ideal candidates for topical and transdermal applications [22, 23].

When a drug is formulated as a nanoemulsion and subsequently transformed into a gel using a gelling agent such as carboxymethyl cellulose (CMC), the resulting hydrogel benefits from the properties of both systems [24, 25]. CMC is a biocompatible and biodegradable polymer known for its excellent water retention, mechanical stability, and mucoadhesive properties, which enhance the effectiveness of the hydrogel formulation [26, 27]. Consequently, the final nanogel retains the advantages of nanoemulsions—such as improved solubility, stability, and drug delivery—while also offering the benefits of hydrogels, including biocompatibility, biodegradability, and ease of topical application [28-30]. In this study, we developed and characterized nanogels loaded with pine EO, bergamot EO, and their mixture and evaluated their antibacterial activity against *E. coli* and *S. aureus*. To the best of our knowledge, this is the first report on the formulation of nanogels containing these specific EOs and the assessment of their antimicrobial potential in such a delivery system.

MATERIALS AND METHODS

Escherichia coli (ATCC 25,922) and *Staphylococcus aureus* (ATCC 25,923) were supplied by the Pasteur Institute of Iran. Carboxymethylcellulose (CMC) and tween 20 were purchased from Merck Chemicals (Germany). The EOs used in this study were purchased from reputable suppliers: *Citrus bergamia* Risso EO was obtained from Zardband Pharmaceuticals Company (Tehran, Iran), and *Pinus sylvestris* EO was provided by Dr. Soleimani's Pharmaceutical Company (Tehran, Iran).

Characterization of bergamot and pine EOs by gas chromatography-mass spectrometry analysis (GC-MS)

Gas chromatographic analysis was conducted using an Agilent 6890 gas chromatograph equipped with a BPX5 capillary column (30 m length, 0.25 mm inner diameter, and 0.25 µm layer thickness). The sample was diluted with n-hexane for component identification and injected (1 µL) into the instrument. The column temperature program was as follows: the initial oven temperature was set at 50 °C and held for 5 minutes, then increased at a rate of 3 °C per minute to 240 °C, followed by a ramp of 15 °C per minute to 300 °C, and held for 3 minutes, resulting in a total run time of 75 minutes. The injector temperature was 250 °C in split mode (1:35), with helium as the carrier gas at a 0.5 ml/min flow rate. The mass spectrometer was an Agilent 5973, operated in electron ionization mode with an ionization voltage of 70 electron volts (eV) and an ion source temperature of 220 °C. The mass scan range was set between 40 and 500 m/z, and data analysis was performed using ChemStation software. Component identification was achieved

by comparing their retention indices with those in reference databases and articles, as well as mass spectra of standard compounds and the computer library.

Preparation and Characterization of nanogels

A fixed amount of pine EO or bergamot EO (100 µL) or a mixture of pine and bergamot EOs (50:50 µL) were mixed with 150 µL of tween 20 at room temperature for 3 minutes. Distilled water was then added dropwise to reach a final volume of 5000 µL, followed by stirring at room temperature for an additional 40 minutes. The particle size and particle size distribution (SPAN) of the nanoemulsions were measured using a dynamic light scattering (DLS) apparatus (K-One Nano Ltd. Korea). The SPAN was calculated using the formula D90 – D10/ D50. D10, D50, and D90 represent the particle sizes at which 10%, 50%, and 90% of the particles have diameters more minor than the specified values. Nanoemulsions with particle sizes < 200 nm and SPAN < 1 were considered the optimal sample for the preparation of nanogel [31].

The prepared nanoemulsions containing pine EO, bergamot EO, and their mixture (5000 µL) were gelified by adding 175 mg of CMC and then stirred overnight at ambient temperature to complete the gelation process [31]. The viscosity of nanogels at shear rates of 0.1–100 1/s was analyzed by rheometer apparatus (MCR-302, Anton Paar, Austria). Moreover, proper incorporation of pine and bergamot EOs into nanogel was investigated through Attenuated Total Reflectance Fourier-Transform Infrared (ATR-FTIR) spectroscopy (Tensor II, Bruker, Germany). The spectra of pine EO, bergamot EO, blank gel, and nanogels were examined in the 400-4000 cm^{-1} range.

AATCC100 Antimicrobial Method

The AATCC100 method was employed to assess the antibacterial properties of the nanogels. Initially, a suspension of the target bacteria was prepared at a standardized concentration of 0.5 McFarland standard (equivalent to 1.5 x 10^8 CFU/ mL). Subsequently, specific quantities of the samples (1000, 500, and 250 milligrams) were added to the bacterial suspension (5 mL). Given that the EO concentration in the nanogel was 10,000 µg/mL, these additions resulted in testing antimicrobial activity at concentrations of 2000, 1000, and 500 µg/mL. After adding the samples, the mixture tubes were incubated at 37°C for 24 hours. Finally, 10 µL of the sample suspension was cultured to Mueller-Hinton agar plates and incubated for 24 hours to determine the growth rate. After the incubation period, the colonies on the plates were counted, and the growth reduction compared to the control group was calculated using the following formula:

Bacterial Growth Percentage = CFU sample / CFU control × 100

RESULTS

Chemical composition of bergamot and pine EOs

The chemical composition of bergamot and pine EOs are listed in Tables 1 and 2, respectively. GC-MS analysis of bergamot EO revealed the identification of 98% of its components, comprising 12 distinct compounds. Among these, the five major compounds were linalool (48.50%), limonene (21.24%), linalool acetate (17.37%), α-terpineol (5.70%), and geranyl acetate (1.74%), which collectively represent the majority of the bergamot EO composition. The constituents of pine EO were fully identified through GC-MS analysis, encompassing seven distinct compounds. Among these, the five major components were α-terpineol (66.69%), ɣ-terpineol (13.10%), terpinen-1-ol (11.15%), cis-β-terpineol (3.00%), and terpinen-4-ol (2.09%), collectively accounting for the majority of the pine EO composition.

Characterization

The DLS diagrams of nanoemulsions are depicted in Figure 1A-C. The particle size of bergamot EO, pine EO, and their mixture were obtained as 34 ± 4 nm, 10 ± 2 nm, and 42 ± 6 nm, respectively. SPAN of bergamot EO, pine EO, and their mixture were measured at 0.97, 0.99, and 0.97, respectively.

The successful loading of bergamot and pine extract into the nanogel structure is verified by ATR-FTIR spectroscopy. The resulting spectra in the wave number range of 400-4000 cm^{-1} are illustrated in Figure 2. The spectrum of bergamot EO displays a broad absorption band centered at 3427 cm^{-1}, characteristic of hydrogen-bonded O-H. This suggests the presence of alcoholic compounds in the extract, especially linalool and α-terpineol. Strong absorption bands in the 2980-2865 cm^{-1} region result from stretching vibrations of aliphatic hydrocarbons. Weaker bands at 3090 and 2743 cm^{-1} indicate the presence of olefinic and aldehydic C-H groups, respectively. The intense band at 1739 cm^{-1}

Table 1. Chemical composition of bergamot EO determined by GC-MS analysis

NO	RT	%	Components	KI	Type
1	11.34	0.86	α-pinene	939	MH[1]
2	13.67	0.74	β-pinene	979	MH
3	14.25	0.53	β-myrcene	991	MH
4	15.24	0.20	δ-3-carene	1011	MH
5	16.40	21.24	limonene	1029	MH
6	20.22	48.50	linalool	1097	MO[2]
7	21.88	0.53	linalool acetate <dihydro->	1275	MO
8	24.31	0.27	terpinene-4-ol	1177	MO
9	25.11	5.70	α-terpineol	1188	MO
10	25.29	0.63	ɣ-terpineol	1199	MO
11	27.35	17.37	linalool acetate	1257	MO
12	33.25	1.74	geranyl acetate	1381	MO
		98.00	total identified		

[1]Monoterpene Hydrocarbons and [2]Oxygenated Monoterpenes

Table 2. Chemical composition of pine EO determined by GC-MS analysis

NO	RT	%	Components	KI	Type
1	21.26	1.95	fenchol <endo->	1116	MO
2	22.03	11.15	terpinene-1-ol	1142	MO
3	22.81	3.00	cis-β-terpineol	1144	MO
4	23.97	2.02	borneol	1169	MO
5	24.32	2.09	terpinene-4-ol	1177	MO
6	25.12	66.69	α-terpineol	1188	MO
7	25.30	13.10	ɣ-terpineol	1199	MO
		100.00	total identified		

indicates the presence of carbonyl compounds, including linalool acetate and geranyl acetate. Additionally, bands at 1645, 1448, and 1372 cm^{-1} can be assigned to C=C stretching, C-O-H bending, and CH_3/CH_2 bending vibrations, respectively. The 1245 and 831 cm^{-1} regions exhibit characteristic bands associated with C-O stretching and out-of-plan (oop) C-H bending vibrations of alkenes and aromatic structures.

The spectrum of pine EO exhibits a strong and broad band centered at 3333 cm^{-1}, suggesting the presence of alcoholic compounds within the extract, especially α-terpineol, ɣ-terpineol, terpinen-1-ol, cis-β-terpineol, terpinen-4-ol, borneol, and fenchol. The C-H and C=C stretching vibrations are observed at 2970-2858 and 1657 cm^{-1}, respectively. Bending vibrations attributed to C-O-H, CH_2 and CH_3 groups are detected at 1452, 1417, 1376, and 1327 cm^{-1}. Intense and sharp absorption bands in the 1140-989 cm^{-1} region are assigned to C-O stretching. The other bands are 927-802 cm^{-1}, resulting from =C-H bending vibrations (oop).

The characteristic absorption bands of CMC are observed at approximately 3331 cm^{-1}, corresponding to O-H stretching vibrations. Peaks at 2923 and 1595 cm^{-1} are attributed to C-H stretching and COO^- asymmetric stretching vibrations, respectively. Additionally, 1418 and 1325 cm^{-1} peaks are associated with CH_2 bending,

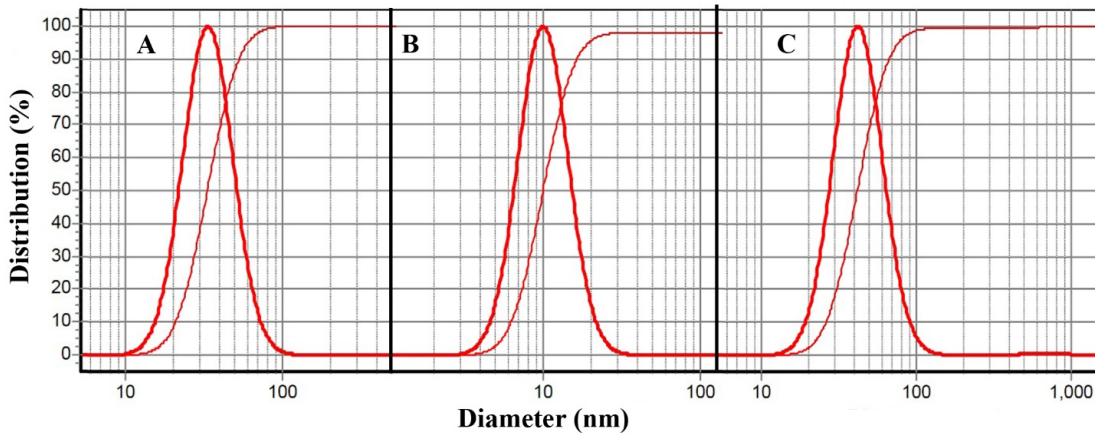

Fig. 1. DLS analysis of A: nanoemulsion containing bergamot EO, B: pine EO, and the mixture of bergamot and pine EOs

COO^- symmetric stretching, and CH_3 bending vibrations, respectively. A prominent and sharp absorption band at 1017 cm^{-1} is assigned to the C-O-C stretching vibrations, characteristic of the glycosidic linkage.

The spectrum of blank gel provides valuable insights into the chemical composition of this nanocarrier. The broad band centered at 3496 cm^{-1} corresponds to the stretching vibrations of O-H groups from CMC and polyoxymethylene chain of tween 20. Medium peaks at 3070-2908 cm^{-1} result from C-H bonds' stretching vibrations. The weak peak at 1744 cm^{-1} is characteristic of the ester carbonyl group in tween 20. A strong peak of around 1583 cm^{-1} corresponds to the carboxylate groups (COO^-) present in the CMC. Medium absorption at 1431 and 1325 cm^{-1} are probably due to CH_2 bending, COO^- symmetric stretching, and CH_3 bending vibrations, respectively. Moreover, a strong peak at 1032 cm^{-1} is associated with the C-O-C stretching vibrations in the ester and ether linkages in tween 20 and CMC.

The bergamot nanogel spectrum exhibits characteristic bands corresponding to both nanogel and bergamot EO, confirming the successful encapsulation of bergamot EO within the nanogel structure. The characteristic peaks at 3526, 2925, 1737, 1583, 1454-1329, 1250, 1058-1033, and 924 cm^{-1} are attributed to O-H, C-H, C=O, COO^-, and C=C stretching, C-O-H and CH_2/ CH_3 bending, C-O stretching, and C-H bending vibrations (oop), respectively. A significant increase in C-H absorption and the appearance of a carbonyl peak at 1737 cm^{-1} suggests the interaction between the nanogel matrix and the encapsulated extract components.

The spectrum of pine nanogel indicates the typical absorptions of O-H, C-H, COO^-, C=C, and C-O bonds at 3483, 3090-2876, 1587, 1456, and 1042 cm^{-1}, respectively. Specific peaks' intensity, shape, and position suggest potential nanogel and pine extract interactions. The red shift of the O-H stretching vibration peak indicates the formation of intermolecular hydrogen bonds between the nanogel and the extract components. Enhanced C-H and C-O stretching vibration bands in pine nanogel compared to the blank nanogel confirm the successful loading of pine EO into the nanogel matrix. Moreover, the peaks observed at 932 and 835 cm^{-1} are attributed to the extract components' =C-H bending vibrations (oop).

Spectral analysis of the bergamot-pine (mix) nanogel sample identifies characteristic peaks corresponding both extracts and nanogel matrix at 3479 (O-H), 3079- 2927 (C-H), 1734 (C=O), 1589 (COO^- and C=C), 1451-1244 (C-O-H, CH_2 and CH_3), 1045 (C-O), and 920 (oop C-H) cm^{-1}. The observed shift of the hydroxyl group to a lower frequency suggests the formation of hydrogen bonds between the nanogel and the components of both extracts. The position and relative intensity of C-H and C=O signals, being lower than those in bergamot nanogel and higher than those in pine nanogel, indicate the presence of components from both extracts within the biopolymer matrix. The shape of the peaks at 1451-1321 cm^{-1} and the characteristic peak at 1244 cm^{-1} provide evidence of both extracts within the matrix. The intense absorption band observed at 1045 cm^{-1} corresponds to C-O stretching vibrations from pine and

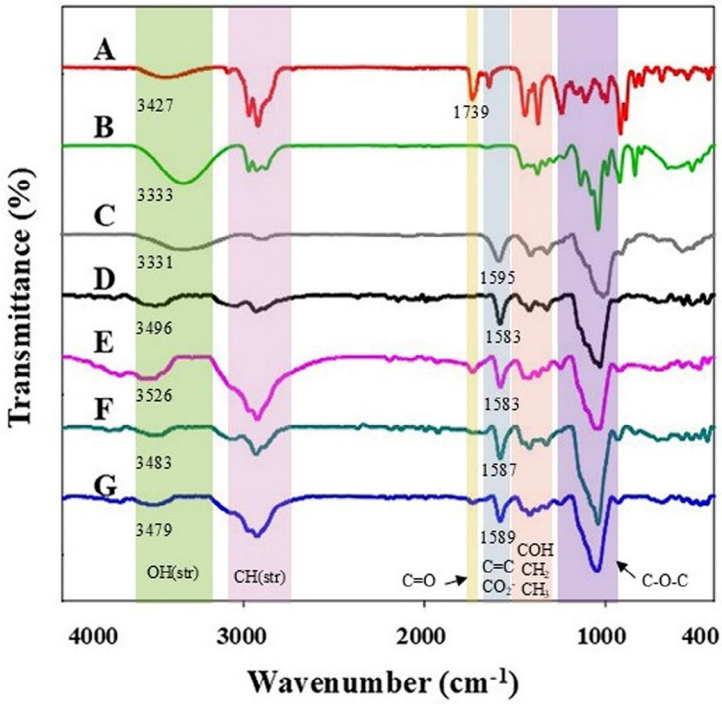

Fig. 2. The ATR-FTIR spectra of A: bergamot EO, B: pine EO, C: CMC, D: blank gel, E: bergamot nanogel, F: pine nanogel, and G: mix nanogel.

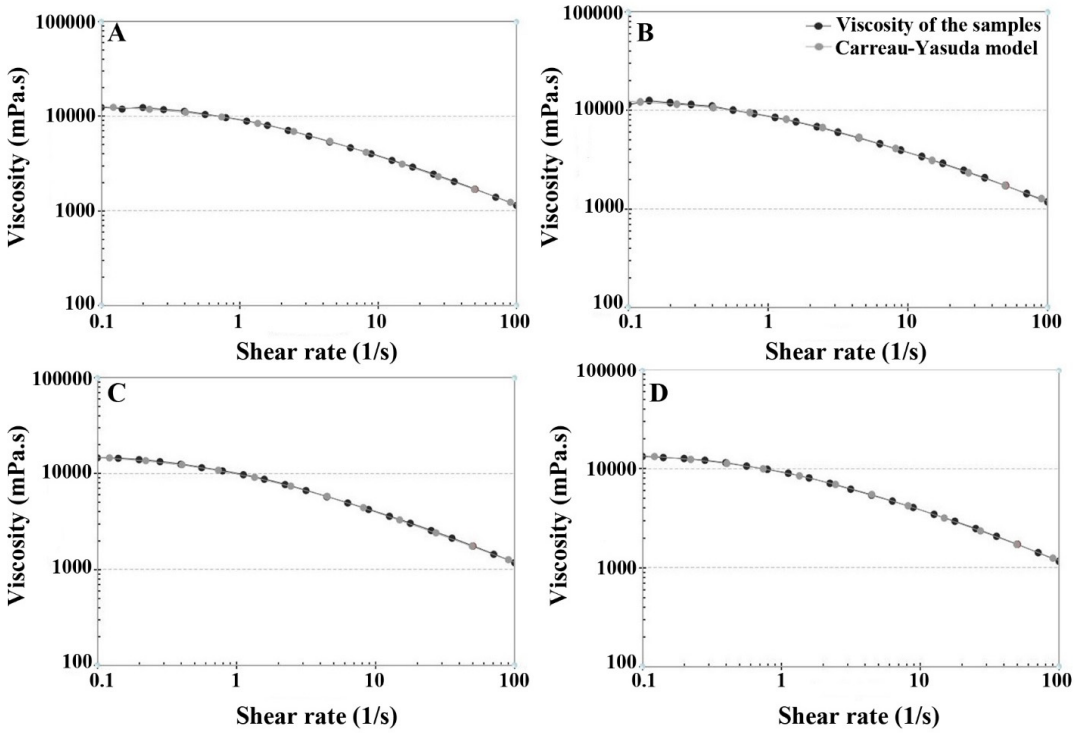

Fig. 3. Viscosity curve of A: blank gel, B: bergamot nanogel, C: pine nanogel, and D: mix nanogel

bergamot components, tween 20 and CMC.

The viscosity profiles of the nanogels are illustrated in Figure 3A-D. Their viscosity at various shear rates is fully fitted to the Carreau-Yasuda model as the well-known regression of non-Newtonian fluids, where the viscosity decreases with a growing shear rate.

Antibacterial evaluation

The antibacterial effect of nanogels against *E. coli* and *S. aureus* at concentrations of 500, 1000, and 2000 µg/mL are shown in Figures 4 and 5. The control group (untreated bacteria) showed 100% growth across all concentrations, confirming normal bacterial proliferation. The blank gel had minimal antibacterial activity, reducing bacterial growth by only 1%– ~10%, indicating that the gel itself did not significantly contribute to bacterial inhibition. For *E. coli*, pine nanogel demonstrated the most potent antibacterial effect, reducing bacterial growth to 5% at 2000 µg/mL. Bergamot nanogel showed moderate efficacy, decreasing *E. coli* growth to 20% at the highest concentration. The mix nanogel exhibited potent antibacterial activity,

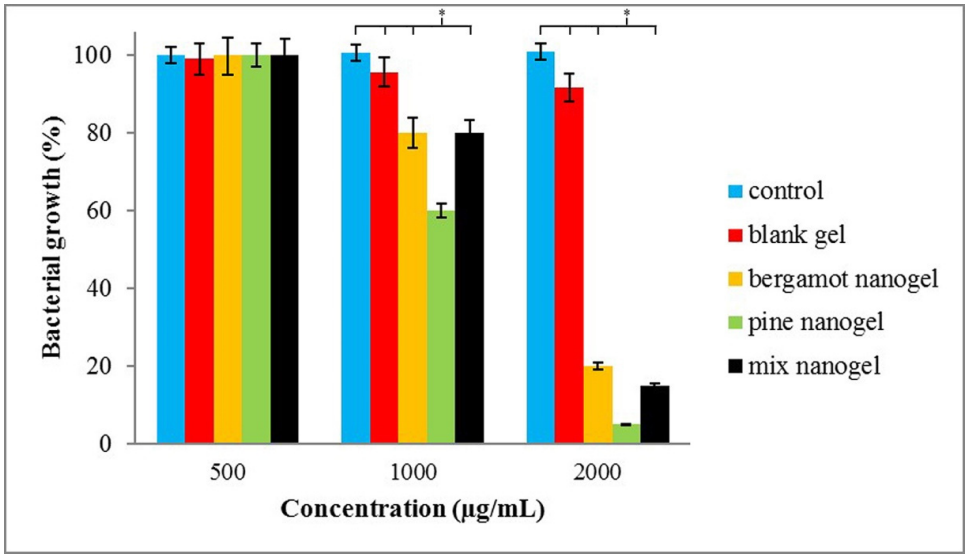

Fig. 4. Antibacterial effects of samples against *E. coli*. * $p < 0.05$

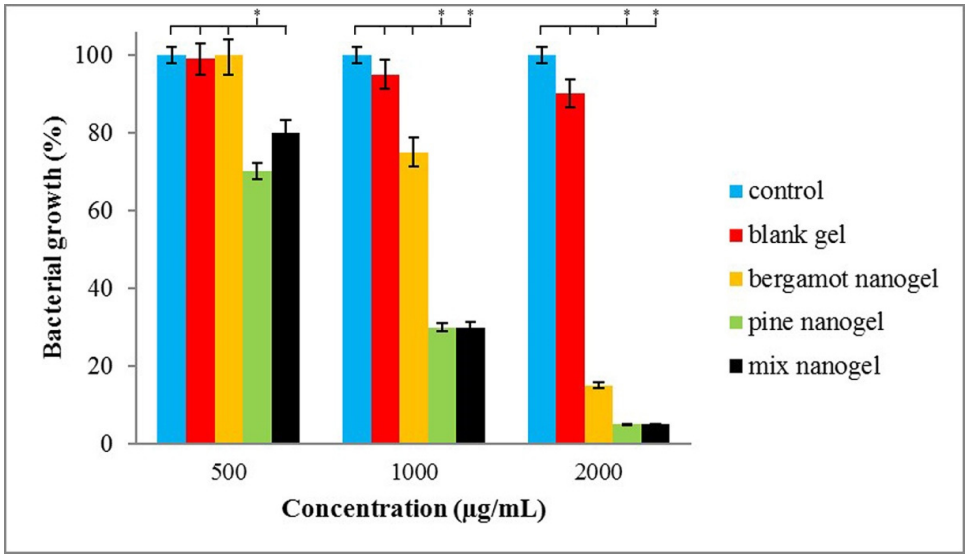

Fig. 5. Antibacterial effects of samples against *S. aureus*. * $p < 0.05$

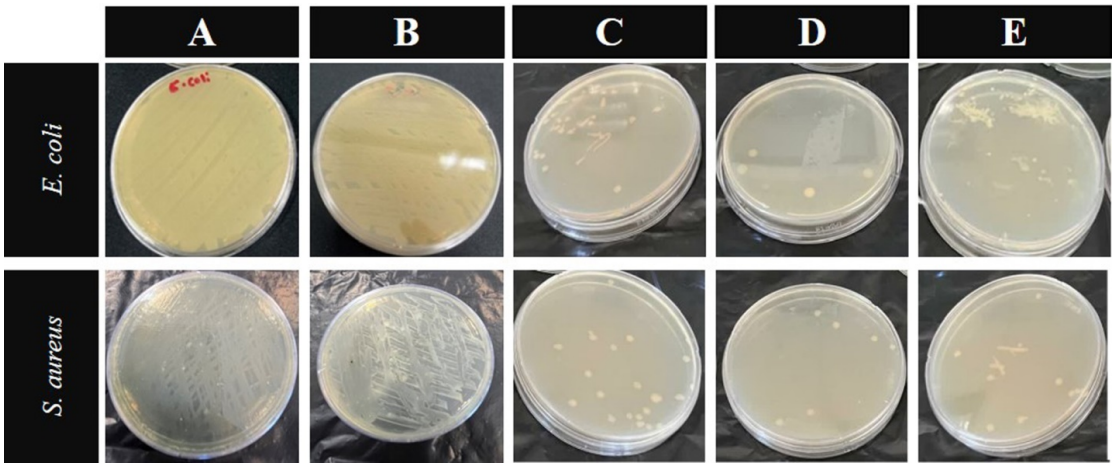

Fig. 6. Examples on cultured plates: A: control, B: blank gel, C: bergamot nanogel, D: pine nanogel, and D: mix nanogel

reducing bacterial growth to 15% at 2000 µg/mL. For *S. aureus*, pine nanogel was the most effective, reducing bacterial growth to 5% at 2000 µg/mL, while bergamot nanogel reduced it to 15%. The mix nanogel displayed a similar inhibitory effect as pine nanogel, with 5% bacterial growth at the highest concentration. Overall, pine nanogel exhibited superior antibacterial activity against *E. coli* and *S. aureus*, followed by the mix nanogel and bergamot nanogel. For better understanding by non-expert readers, a real image example of the grown colonies after treatment with nanogels is presented in Figure 6 from the cultured plates.

DISCUSSION

One of the major threats to human health is antibiotic resistance, primarily from the overuse of antibiotics in humans, animals, and the environment [32]. Plant EOs have emerged as viable alternatives to combat antibiotic-resistant bacteria due to their diverse bioactive compounds, which reduce the likelihood of bacterial adaptation and resistance [33-35]. Nanoformulation of herbal EOs has emerged as a promising approach to enhance their bioavailability, physicochemical properties, high loading capacity, solubility, stability, and targeted drug delivery [36-38]. Therefore, the present study aimed to develop nanogels incorporating bergamot and pine EOs and their mixture and evaluate their antibacterial efficacy and rheological properties.

The antibacterial evaluation of the developed nanogels demonstrated significant efficacy against *E. coli* and *S. aureus*. Pine nanogel exhibited the highest antibacterial activity among the tested formulations, reducing *E. coli* and *S. aureus* growth to 5% at 2000 µg/mL. Bergamot nanogel showed moderate inhibition, while the mix nanogel demonstrated strong antibacterial effects comparable to pine nanogel. The antibacterial assessment was conducted using the AATCC100 method, a widely accepted standard for evaluating antimicrobial textiles and surfaces. Unlike disk diffusion, which only measures the inhibition zone, AATCC100 quantifies bacterial survival post-treatment, providing a more dynamic assessment of antimicrobial efficacy. Additionally, while MIC and MBC determine bacterial inhibition at specific concentrations, AATCC100 allows for evaluating bacterial reduction over time or across varying concentrations. It is beneficial for assessing sustained antimicrobial efficacy in formulations like nanogels [39, 40].

Several studies have reported the potent antibacterial effects of nanoformulated EOs against *S. aureus* and *E. coli*. For example, treatment with polycaprolactone nanofibers containing *Mentha piperita* EO reduced the survival rate of *S. aureus* and *E. coli* by approximately 50% after 24 hours [41]. Additionally, a nanogel containing 1250 µg/mL of *Mentha piperita* EO reduced *S. aureus* growth by 30% and *E. coli* growth by 95% [42]. Furthermore, caraway nanogel exhibited MIC and MBC values of 0.78 mg/mL and 3.125 mg/mL, respectively, against *S. aureus* and *E. coli* [43]. In another study, treatment with 2500 and 5000 µg/mL of nanogel containing *Mentha longifolia* EO resulted in 3% and 100% growth inhibition of *S. aureus*, respectively [44]. Notably, camphor nanogel (2500

μg/mL) completely inhibited the growth of both *S. aureus* and *E. coli*, and thymol nanogel at the same concentration exhibited 100% inhibition against *S. aureus* [45]. These findings align with the current study, reinforcing the potential of nanoformulated EOs in antibacterial applications.

The viscosity analysis demonstrated that the nanogels exhibit non-Newtonian, pseudoplastic behavior, as their flow characteristics conform to the Carreau-Yasuda model. This model effectively describes the shear-thinning behavior of polymer-based gels by accounting for viscosity variations across different shear rates [46, 47]. The observed shear-thinning properties are advantageous in biomedical applications, particularly in topical and injectable drug delivery systems, where high viscosity at rest prevents premature drug release. In contrast, lower viscosity under shear facilitates ease of application or injection. Precise rheological characterization aids in optimizing nanogel formulations for targeted delivery, adhesion, and controlled drug diffusion [48, 49].

Over the years, researchers have extensively investigated the mechanism of action of EOs and their major components. It is widely accepted that the antimicrobial effects of EOs are attributed to their ability to disrupt microbial enzymatic systems involved in energy production and cell membrane synthesis [50, 51]. *Pinus sylvestris* exhibits antibacterial properties against pathogens such as *Neisseria gonorrhoeae* and *Streptococcus suis* due to its bioactive components, including α-pinene, β-pinene, and D-limonene**.** Current evidence suggests that the antibacterial mechanism of *P. sylvestris* is linked to its ability to induce severe cell membrane disruption and biofilm dispersion [52, 53]. Likewise, *Citrus bergamia* EO exerts its antimicrobial activity through the lytic effects of its components on microbial cell membranes. This bactericidal activity of *Citrus bergamia* is primarily attributed to its high limonene content [54, 55].

CONCLUSION

This study successfully formulated nanogels containing bergamot EO, pine EO, and their mixture. Pine nanogel exhibited the most potent antibacterial effect against *E. coli* and *S. aureus*, outperforming the other formulations. With its simple preparation and potent antibacterial properties, pine nanogel is a promising candidate for further research in antimicrobial applications.

DECLARATIONS

Ethics approval and consent to participate

This study has been ethically approved (IR.FUMS.REC.1403.040), and since this research did not involve human study, the informed consent form was thus not used.

Consent for publication

Not applicable.

Acknowledgments

Not applicable

Availability of data and materials

The datasets used and/or analyzed during the current study are available from the corresponding author upon reasonable request.

Competing interests

Not applicable.

Funding

Fasa University of Medical Sciences supported this study grant No. 403031.

Authors' contributions

FD prepared nanoparticles. EA drafted MS in cooperation with MO. RH interpreted ATR-FTIR spectra. ER performed antibacterial assays. ZM revised the MS. MO designed the study, analyzed data, and drafted the manuscript. All authors contributed to drafting and approving the final manuscript.

REFERENCES

1. Udy AA, Roberts JA, Lipman J, Blot S. The effects of major burn related pathophysiological changes on the pharmacokinetics and pharmacodynamics of drug use: An appraisal utilizing antibiotics. Adv Drug Deliv Rev. 2018;123:65-74. https://doi.org/10.1016/j.addr.2017.09.019
2. Singer AJ, Talan DA. Management of skin abscesses in the era of methicillin-resistant Staphylococcus aureus. N Engl J Med. 2014;370(11):1039-47. https://doi.org/10.1056/NEJMra1212788
3. Esposito S, Ascione T, Pagliano P. Management of bacterial skin and skin structure infections with polymicrobial etiology. Expert Rev Anti Infect Ther. 2019;17(1):17-25. https://doi.org/10.1080/14787210.2019.1552518
4. Stevens DL, Bisno AL, Chambers HF, Dellinger P, Goldstein EJ, Gorbach SL, et al. Practice guidelines for the diagnosis and management of skin and soft-tissue infections. Clin Infect Dis. 2005;41(10):1373-406. https://doi.org/10.1086/497143

5. Jenkins A, Diep BA, Mai TT, Vo NH, Warrener P, Suzich J, et al. Differential expression and roles of Staphylococcus aureus virulence determinants during colonization and disease. mBio. 2015;6(1):e02272-14. https://doi.org/10.1128/mBio.02272-14
6. Cho JS, Zussman J, Donegan NP, Ramos RI, Garcia NC, Uslan DZ, et al. Noninvasive in vivo imaging to evaluate immune responses and antimicrobial therapy against Staphylococcus aureus and USA300 MRSA skin infections. J Invest Dermatol. 2011;131(4):907-15. https://doi.org/10.1038/jid.2010.417
7. Deusenbery C, Wang Y, Shukla A. Recent innovations in bacterial infection detection and treatment. ACS Infect Dis. 2021;7(4):695-720. https://doi.org/10.1021/acsinfecdis.0c00890
8. Čurová K, Slebodníková R, Kmeťová M, Hrabovský V, Maruniak M, Liptáková E, et al. Virulence, phylogenetic background and antimicrobial resistance in Escherichia coli associated with extraintestinal infections. J Infect Public Health. 2020;13(10):1537-43. https://doi.org/10.1016/j.jiph.2020.06.032
9. D'Achille G, Morroni G. Side effects of antibiotics and perturbations of mitochondria functions. Int Rev Cell Mol Biol. 2023;377:121-39. https://doi.org/10.1016/bs.ircmb.2023.03.009
10. De Kraker ME, Davey PG, Grundmann H; BURDEN Study Group. Mortality and hospital stay associated with resistant Staphylococcus aureus and Escherichia coli bacteremia: estimating the burden of antibiotic resistance in Europe. PLoS Med. 2011;8(10):e1001104. https://doi.org/10.1371/journal.pmed.1001104
11. Collignon P. Antibiotic resistance: are we all doomed? Intern Med J. 2015;45(11):1109-15. https://doi.org/10.1111/imj.12902
12. Mandal J, Acharya NS, Buddhapriya D, Parija SC. Antibiotic resistance pattern among common bacterial uropathogens with a special reference to ciprofloxacin resistant Escherichia coli. Indian J Med Res. 2012;136(5):842-9.
13. Ocsoy I, Tasdemir D, Mazicioglu S, Tan W. Nanotechnology in plants. In: Plant genetics and molecular biology. 2018:263-75. https://doi.org/10.1007/10_2017_53
14. Dzotam JK, Simo IK, Bitchagno G, Celik I, Sandjo LP, Tane P, et al. In vitro antibacterial and antibiotic modifying activity of crude extract, fractions and 3′,4′,7-trihydroxyflavone from Myristica fragrans Houtt against MDR Gram-negative enteric bacteria. BMC Complement Altern Med. 2018;18:1-9. https://doi.org/10.1186/s12906-018-2084-1
15. Navarra M, Ferlazzo N, Cirmi S, Trapasso E, Bramanti P, Lombardo GE, et al. Effects of bergamot essential oil and its extractive fractions on SH-SY5Y human neuroblastoma cell growth. J Pharm Pharmacol. 2015;67(8):1042-53. https://doi.org/10.1111/jphp.12403
16. Mandalari G, Bennett RN, Bisignano G, Trombetta D, Saija A, Faulds CB, et al. Antimicrobial activity of flavonoids extracted from bergamot (Citrus bergamia Risso) peel, a byproduct of the essential oil industry. J Appl Microbiol. 2007;103(6):2056-64. https://doi.org/10.1111/j.1365-2672.2007.03456.x
17. Sharma A, Goyal R, Sharma L. Potential biological efficacy of Pinus plant species against oxidative, inflammatory and microbial disorders. BMC Complement Altern Med. 2015;16:1-11. https://doi.org/10.1186/s12906-016-1011-6
18. Ács K, Balázs VL, Kocsis B, Bencsik T, Böszörményi A, Horváth G. Antibacterial activity evaluation of selected essential oils in liquid and vapor phase on respiratory tract pathogens. BMC Complement Altern Med. 2018;18:1-9. https://doi.org/10.1186/s12906-018-2291-9
19. Herman RA, Ayepa E, Shittu S, Fometu SS, Wang J. Essential Oils and their applications-A mini review. Adv Nutr Food Sci. 2019;4(4):1-13.
20. Kersey FR, Merkel TJ, Perry JL, Napier ME, DeSimone JM. Effect of aspect ratio and deformability on nanoparticle extravasation through nanopores. Langmuir. 2012;28(23):8773-81. https://doi.org/10.1021/la301279v
21. Rolland JP, Maynor BW, Euliss LE, Exner AE, Denison GM, DeSimone JM. Direct fabrication and harvesting of monodisperse, shape-specific nanobiomaterials. J Am Chem Soc. 2005;127(28):10096-100. https://doi.org/10.1021/ja051977c
22. Bastos LPH, Vicente J, dos Santos CHC, de Carvalho MG, Garcia-Rojas EE. Encapsulation of black pepper (Piper nigrum L.) essential oil with gelatin and sodium alginate by complex coacervation. Food Hydrocoll. 2020;102:105605. https://doi.org/10.1016/j.foodhyd.2019.105605
23. Donsì F, Ferrari G. Essential oil nanoemulsions as antimicrobial agents in food. J Biotechnol. 2016;233:106-20. https://doi.org/10.1016/j.jbiotec.2016.07.005
24. Kabanov AV, Vinogradov SV. Nanogels as pharmaceutical carriers: finite networks of infinite capabilities. Angew Chem Int Ed Engl. 2009;48(30):5418-29. https://doi.org/10.1002/anie.200900441
25. Torchilin VP. Multifunctional, stimuli-sensitive nanoparticulate systems for drug delivery. Nat Rev Drug Discov. 2014;13(11):813-27. https://doi.org/10.1038/nrd4333
26. Rahman MS, Hasan MS, Nitai AS, Nam S, Karmakar AK, Ahsan MS, et al. Recent Developments of Carboxymethyl Cellulose. Polymers (Basel). 2021;13(8):[article number]. https://doi.org/10.3390/polym13081345
27. Zennifer A, Senthilvelan P, Sethuraman S, Sundaramurthi D. Key advances of carboxymethyl cellulose in tissue engineering & 3D bioprinting applications. Carbohydr Polym. 2021;256:117561. https://doi.org/10.1016/j.carbpol.2020.117561
28. Qiao ZY, Zhang R, Du FS, Liang DH, Li ZC. Multi-responsive nanogels containing motifs of ortho ester, oligo(ethylene glycol) and disulfide linkage as carriers of hydrophobic anti-cancer drugs. J Control Release. 2011;152(1):57-66. https://doi.org/10.1016/j.jconrel.2011.02.029
29. Hayashi C, Hasegawa U, Saita Y, Hemmi H, Hayata T, Nakashima K, et al. Osteoblastic bone formation is induced by using nanogel-crosslinking hydrogel as novel scaffold for bone growth factor. J Cell Physiol. 2009;220(1):1-7. https://doi.org/10.1002/jcp.21760
30. Hasegawa U, Shin-ichiro MN, Kaul SC, Hirano T, Akiyoshi K. Nanogel-quantum dot hybrid nanoparticles for live cell imaging. Biochem Biophys Res Commun. 2005;331(4):917-21. https://doi.org/10.1016/j.bbrc.2005.03.228
31. Abdollahi A, Fereydouni N, Moradi H, Karimivaselabadi A, Zarenezhad E, Osanloo M. Nanoformulated herbal compounds: enhanced antibacterial efficacy of camphor and thymol-loaded nanogels. BMC Complement Med Ther. 2024;24(1):138. https://doi.org/10.1186/s12906-024-04435-z

32. Ding D, Wang B, Zhang X, Zhang J, Zhang H, Liu X, et al. The spread of antibiotic resistance to humans and potential protection strategies. Ecotoxicol Environ Saf. 2023;254:114734. https://doi.org/10.1016/j.ecoenv.2023.114734
33. Trifan A, Luca SV, Greige-Gerges H, Miron A, Gille E, Aprotosoaie AC. Recent advances in tackling microbial multidrug resistance with essential oils: Combinatorial and nano-based strategies. Crit Rev Microbiol. 2020;46(3):338-57. https://doi.org/10.1080/1040841X.2020.1782339
34. Wińska K, Mączka W, Łyczko J, Grabarczyk M, Czubaszek A, Szumny A. Essential oils as antimicrobial agents-myth or real alternative? Molecules. 2019;24(11):2130. https://doi.org/10.3390/molecules24112130
35. Zouhir A, Jridi T, Nefzi A, Ben Hamida J, Sebei K. Inhibition of methicillin-resistant Staphylococcus aureus (MRSA) by antimicrobial peptides (AMPs) and plant essential oils. Pharm Biol. 2016;54(12):3136-50. https://doi.org/10.1080/13880209.2016.1190763
36. Woranuch S, Yoksan R. Eugenol-loaded chitosan nanoparticles: I. Thermal stability improvement of eugenol through encapsulation. Carbohydr Polym. 2013;96(2):578-85. https://doi.org/10.1016/j.carbpol.2012.08.117
37. Zanetti M, Carniel TK, Dalcanton F, dos Anjos RS, Riella HG, de Araújo PH, et al. Use of encapsulated natural compounds as antimicrobial additives in food packaging: A brief review. Trends Food Sci Technol. 2018;81:51-60. https://doi.org/10.1016/j.tifs.2018.09.003
38. Swain SS, Paidesetty SK, Padhy RN, Hussain T. Nanotechnology platforms to increase the antibacterial drug suitability of essential oils: A drug prospective assessment. OpenNano. 2023;9:100115. https://doi.org/10.1016/j.onano.2022.100115
39. Hossain TJ. Methods for screening and evaluation of antimicrobial activity: A review of protocols, advantages, and limitations. Eur J Microbiol Immunol (Bp). 2024;14(2):97-115. https://doi.org/10.1556/1886.2024.00035
40. Balouiri M, Sadiki M, Ibnsouda SK. Methods for in vitro evaluating antimicrobial activity: A review. J Pharm Anal. 2016;6(2):71-9. https://doi.org/10.1016/j.jpha.2015.11.005
41. Unalan I, Slavik B, Buettner A, Goldmann WH, Frank G, Boccaccini AR. Physical and antibacterial properties of peppermint essential oil loaded poly(ε-caprolactone) (PCL) electrospun fiber mats for wound healing. Front Bioeng Biotechnol. 2019;7:346. https://doi.org/10.3389/fbioe.2019.00346
42. Sanei-Dehkordi A, Abdollahi A, Safari M, Karami F, Ghaznavi G, Osanloo M. Nanogels containing Foeniculum vulgare Mill. and Mentha piperita L. essential oils: Mosquitoes' repellent activity and antibacterial effect. Interdiscip Perspect Infect Dis. 2022;2022:4510182. https://doi.org/10.1155/2022/4510182
43. Alqarni MH, Foudah AI, Aodah AH, Alkholifi FK, Salkini MA, Alam A. Caraway Nanoemulsion Gel: A Potential Antibacterial Treatment against Escherichia coli and Staphylococcus aureus. Gels. 2023;9(3):193. https://doi.org/10.3390/gels9030193
44. Qasemi H, Fereidouni Z, Karimi J, Abdollahi A, Zarenezhad E, Rasti F, et al. Promising antibacterial effect of impregnated nanofiber mats with a green nanogel against clinical and standard strains of Pseudomonas aeruginosa and Staphylococcus aureus. J Drug Deliv Sci Technol. 2021;66:102844. https://doi.org/10.1016/j.jddst.2021.102844
45. Abdollahi A, Fereydouni N, Moradi H, Karimivaselabadi A, Zarenezhad E, Osanloo M. Nanoformulated herbal compounds: enhanced antibacterial efficacy of camphor and thymol-loaded nanogels. BMC Complement Med Ther. 2024;24(1):138. https://doi.org/10.1186/s12906-024-04435-z
46. Coclite A, Coclite GM, De Tommasi D. Capsules Rheology in Carreau-Yasuda Fluids. Nanomaterials (Basel). 2020;10(11):[article number]. https://doi.org/10.3390/nano10112190
47. Hou E, Wang F. Computational Assessment of Thermal and Solute Mechanisms in Carreau-Yasuda Hybrid Nanoparticles Involving Soret and Dufour Effects over Porous Surface. Micromachines (Basel). 2021;12(11):[article number]. https://doi.org/10.3390/mi12111302
48. Bashir S, Ramzan M, Chung JD, Chu YM, Kadry S. Analyzing the impact of induced magnetic flux and Fourier's and Fick's theories on the Carreau-Yasuda nanofluid flow. Sci Rep. 2021;11(1):9230. https://doi.org/10.1038/s41598-021-87831-6
49. Ranjbar R, Zarenezhad E, Abdollahi A, Nasrizadeh M, Firooziyan S, Namdar N, et al. Nanoemulsion and Nanogel Containing Cuminum cyminum L Essential Oil: Antioxidant, Anticancer, Antibacterial, and Antilarval Properties. J Trop Med. 2023;2023:5075581. https://doi.org/10.1155/2023/5075581
50. Patra JK, Baek KH. Antibacterial Activity and Action Mechanism of the Essential Oil from Enteromorpha linza L. against Foodborne Pathogenic Bacteria. Molecules. 2016;21(3):388. https://doi.org/10.3390/molecules21030388
51. Chouhan S, Sharma K, Guleria S. Antimicrobial Activity of Some Essential Oils-Present Status and Future Perspectives. Medicines (Basel). 2017;4(3):[article number]. https://doi.org/10.3390/medicines4030058
52. Omidbeygi M, Barzegar M, Hamidi Z, Naghdibadi H. Antifungal activity of thyme, summer savory and clove essential oils against Aspergillus flavus in liquid medium and tomato paste. Food Control. 2007;18(12):1518-23. https://doi.org/10.1016/j.foodcont.2006.12.003
53. Jurado P, Uruén C, Martínez S, Lain E, Sánchez S, Rezusta A, et al. Essential oils of Pinus sylvestris, Citrus limon and Origanum vulgare exhibit high bactericidal and anti-biofilm activities against Neisseria gonorrhoeae and Streptococcus suis. Biomed Pharmacother. 2023;168:115703. https://doi.org/10.1016/j.biopha.2023.115703
54. Cirmi S, Bisignano C, Mandalari G, Navarra M. Anti-infective potential of Citrus bergamia Risso et Poiteau (bergamot) derivatives: a systematic review. Phytother Res. 2016;30(9):1404-11. https://doi.org/10.1002/ptr.5646
55. Quirino A, Morelli P, Capua G, Arena G, Matera G, Liberto MC, et al. Synergistic and antagonistic effects of Citrus bergamia distilled extract and its major components on drug resistant clinical isolates. Nat Prod Res. 2020;34(11):1626-9. https://doi.org/10.1080/14786419.2018.1522631